ARTICLE TYPE www.rsc.org/xxxxxx | XXXXXXXX

Relativistic effects in metallocorroles: Comparison of molybdenum and tungsten biscorroles

Abraham B. Alemayehu,[a] Hugo Vazquez-Lima,[a] Laura J. McCormick[b] and Abhik Ghosh*[a]

Received (in XXX, XXX) Xth XXXXXXXXX 20XX, Accepted Xth XXXXXXXXX 20XX
DOI: 10.1039/b000000x

The homoleptic sandwich compounds – Mo and W biscorroles – have afforded a novel platform for experimental studies of relativistic effects. A 200-mV difference in reduction potential and a remarkable 130-nm shift of a near-IR spectral feature have been identified as manifestations of relativistic effects on the properties of these complexes.

Detailed comparative studies of analogous 4d and 5d transition metal complexes can potentially provide insights into the importance of relativistic effects.[1,2,3,4,5,6] Yet, there have been relatively few such studies on typical inorganic and organometallic complexes[7,8,9] and no more than a couple on metalloporphyrins and related complexes.[10] Important opportunities in this regard are provided by recent syntheses of several 5d metallocorroles,[11,12,13,14,15,16,17,18] which have garnered attention as unique size-mismatched complexes combining a large 5d transition metal and a sterically constrained corrole ligand. Thus, in a recent study, we were able to attribute a ~28-nm redshift in the Soret maxima of rhenium(V)-oxo corroles, relative to analogous technetium(V)-oxo corroles, to relativistic effects.[19] Molybdenum biscorroles, reported herein, and their tungsten analogues, reported previously,[20] now provide an opportunity for experimental studies of relativistic effects in these unique Group 6 sandwich compounds.

The synthetic coordination chemistry of Mo and W corroles already points to significant chemical differences between the two metals. Whereas the high-temperature interaction of $Mo(CO)_6$ and a free-base *meso*-tris(*p*-X-phenyl)corrole, H_3[T*p*XPC], readily affords Mo^{V}[T*p*XPC]O,[21] the corresponding $W^{V}O$ complexes are unknown.[22] Instead, upon refluxing in decalin in the presence of K_2CO_3, $W(CO)_6$ and H_3[T*p*XPC] were found to yield W[T*p*XPC]$_2$ (X = CF_3, H, Me), the only examples of homoleptic corrole sandwich compounds reported to date.[14] While the reason underlying the elusiveness of $W^{V}O$ corroles remains unclear, we conjectured that the interaction of H_3[T*p*XPC] and $Mo(CO)_6$ under strict exclusion of oxygen might afford Mo biscorroles. Indeed, upon prolonged heating (186 °C, 16 h) in decalin under anerobic conditions, the interaction of H_3[T*p*XPC], $Mo(CO)_6$, and K_2CO_3 afforded, after work-up, 25-30% yields of Mo[T*p*XPC]$_2$ along with 15-20% yields of Mo^{V}[T*p*XPC]O, where X = H, Me, OMe. As delineated below,

Table 1. Soret and Q maxima (nm), redox potentials (V), and electrochemical HOMO-LUMO gaps (V) of M[T*p*XPC]$_2$ (M = Mo, W) as a function of X.

X	UV-vis		$E_{1/2ox2}$	$E_{1/2ox1}$	$E_{1/2red1}$	$E_{1/2red2}$	D*E*
Molybdenum							
H	356	908	0.72	0.23	-0.83	-1.78	1.06
Me	362	909	0.67	0.18	-0.88	-1.84	1.06
OMe	350	909	0.66	0.19	-0.89	-1.85	1.08
Tungsten							
CF_3	356	778	0.88	0.45	-0.88	-1.71	1.33
H	357	781	0.75	0.25	-1.07	-1.79	1.32
Me	359	783	0.72	0.21	-1.11	-1.82	1.32

electrochemical and UV-vis measurements indeed reveal muliple differences between Mo and W biscorroles that may be ascribed to relativistic effects (Table 1).

As with the previously reported W biscorroles,[14] the ^{1}H NMR spectra (including variable temperature experiments) of Mo[T*p*XPC]$_2$ exhibited strongly overlapping peaks in the aromatic region, which defied assignment. For X = Me and OMe, however, the aliphatic regions exhibited three equally intense methyl signals, consistent with C_1 local symmetry of the individual corroles and overall C_2 symmetry of the complexes. Fortunately, one of the complexes, Mo[T*p*MePC]$_2$, proved amenable to single-crystal X-ray diffraction analysis (Figure 1), allowing a detailed structural comparison of the Mo and W complexes.[23] Thus, both metals exhibit square antiprism coordination geometries and essentially identical M-N distances of ~2.2 Å and M-N_4 displacements of 1.18 Å.

The Mo[T*p*XPC]$_2$ derivatives exhibit two reversible oxidations and one reversible reduction in CH_2Cl_2 (Figure 2). As shown in Table 1, for a given *para* substituent X, the first oxidation potentials of Mo and W biscorroles are essentially identical. The first reduction potentials of Mo biscorroles on the other hand are some 200 mV higher than those of their W counterparts. The more negative reduction potentials of the W biscorroles relative to Mo raise the question whether the difference arises, to a

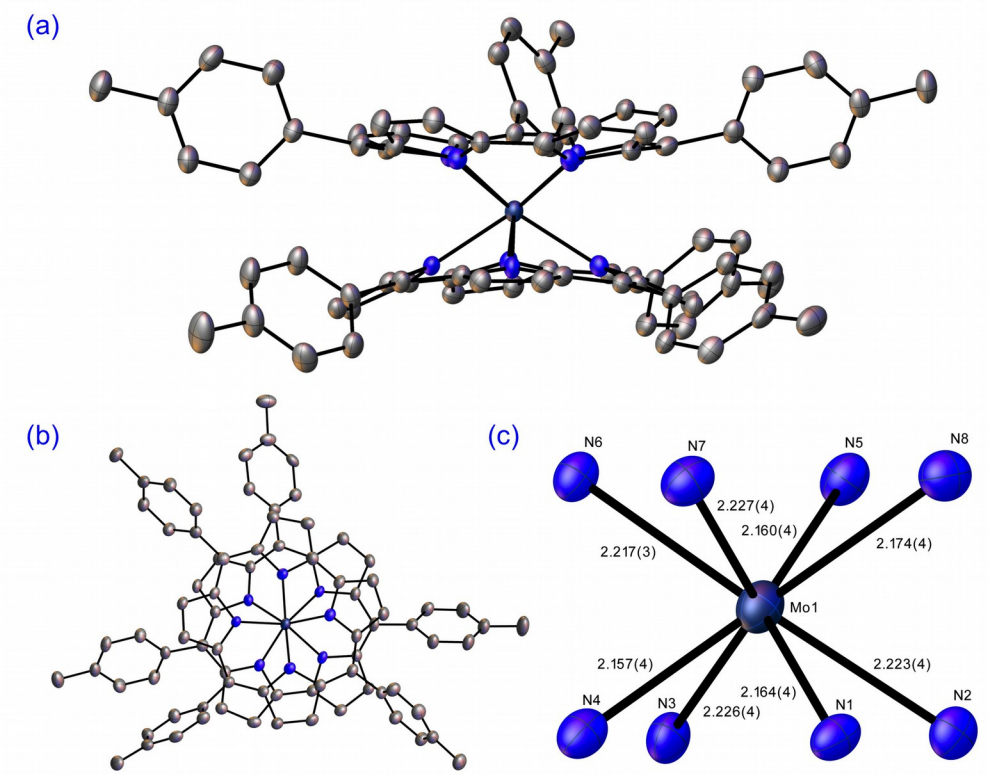

Figure 1. Thermal ellipsoid (50%) plots for Mo[T*p*MePC]$_2$: (a) side and (b) top views; (c) Mo-N distances (Å).

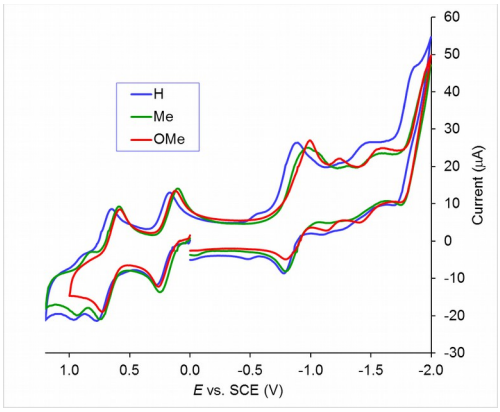

Figure 2. Cyclic voltammograms of Mo[T*p*XPC]$_2$ (X = H, Me and OMe).

significant extent, from relativistic effects. As described below, DFT calculations were used to investigate the nature of this difference.

Like their W congeners, the Mo biscorroles exhibit distinctive UV-vis spectra, including both a hypsochromically shifted Soret band at 356 ± 6 nm and near-IR Q-like bands (Figure 3). The two metals also exhibit key differences. The Soret bands of all three Mo corroles synthesized exhibit a second, sharp peak or shoulder at 424 ± 4 nm; the analogous peak for W biscorroles is much weaker. Also, the Mo biscorroles exhibit two distinct near-IR features in the 750-1000 nm region; the lower-energy feature at 908-909 nm is dramatically redshifted (by some 130 nm) relative to the near-IR feature of W biscorroles.

The above differences between Mo and W corroles were investigated with DFT and TDDFT calculations,[24,25] with relativistic effects taken into account with the zeroth order regular approximation (ZORA) to the two-component Dirac equation applied as a scalar correction. Use of a nonrelativistic Hamiltonian in all-electron B3LYP/STO-TZP calculations resulted in nearly identical HOMO and LUMO orbital energies, ionization potentials and electron affinities for Mo[TPC]$_2$ and W[TPC]$_2$. Deploying the ZORA Hamiltonian upshifted the LUMO orbital energy of W[TPC]$_2$ by ~200 meV, relative to a nonrelativistic Hamiltonian, but had a much smaller impact on Mo[TPC]$_2$. The same effect was also reproduced with DSCF calculations of electron affinities, where the ZORA Hamiltonian decreased the electron affinity of W[TPC]$_2$, relative to a nonrelativistic Hamiltonian, by ~170 meV.[26,27] For both Mo[TPC]$_2$ and W[TPC]$_2$, the LUMO has substantial metal(d_{z^2}) character (Figure 4), which explains why it should be relativistically destabilized in W case. Thus, the ~200 mV difference in reduction potentials between the Mo[T*p*XPC]$_2$ and W[T*p*XPC]$_2$ series is largely attributable to relativistic effects in the W series.

Relativistic ZORA TDDFT (CAMY[28]-B3LYP/STO-TZP/COSMO; solvent = CH_2Cl_2) calculations readily assigned the lowest-energy near-IR feature of both Mo[TPC]$_2$ and W[TPC]$_2$ to a (HOMO – 1)→LUMO transition (Figure 4). Comparison with TDDFT calculations, which employed a nonrelativistic Hamiltonian but an otherwise identical set of computational parameters, clearly implicated relativistic destabilization of the $5d_{z^2}$ orbital of W as the major contributor to the higher energy of this transition in the W case or, equivalently,

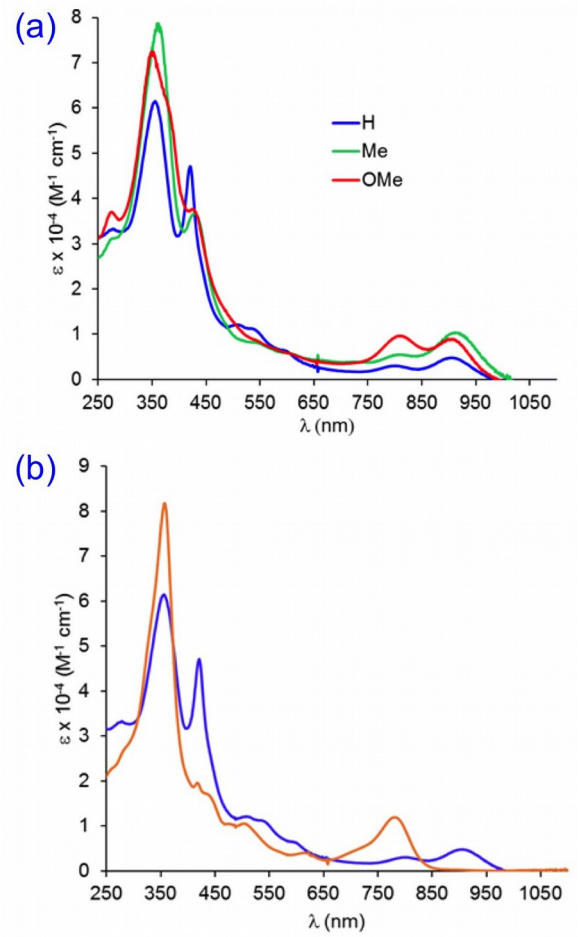

Figure 3. UV vis spectra of (a) Mo[T*p*XPC]$_2$ (X = H, Me and OMe) and of (b) Mo[TPC]$_2$ (blue) and W[TPC]$_2$ (orange).

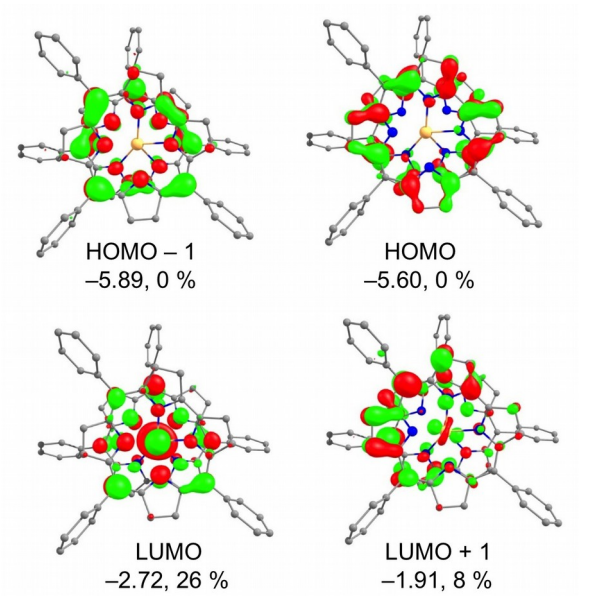

Figure 4. Selected frontier MOs and Mo[TPC]$_2$ along with their orbital energies (eV) and % d character.

to the dramatic redshift observed in the Mo case. The calculations did not, however, provide an assignment for the second, higher-energy near-IR feature of the Mo biscorroles, which suggests that it may be a combination/vibronic band. No significant relativistic effect was found for the Soret band position of Mo[TPC]$_2$ and W[TPC]$_2$, in apparent agreement with the near-identical Soret maxima observed experimentally for both compounds (Figure 3).

Conclusions

As the sole representatives of homoleptic corrole sandwich compounds, Mo and W biscorroles provide a novel platform for experimental studies of relativistic effects. X-ray crystallographic analyses have shown that the two metals exhibit near-identical M-N distances (~2.2 Å) and M-N$_4$ displacements (~1.18 Å). The Mo complexes exhibit distinctly higher reduction potentials (i.e., are easier to reduce), by a margin of ~200 mV, than the analogous W complexes. The UV-vis spectra of Mo biscorroles also exhibit a near-IR feature at 908-909 nm, which is redshifted by some 130 nm relative to an analogous feature of W biscorroles. TDDFT calculations have identified this feature as a (HOMO – 1)→LUMO transition. For both the Mo and W biscorroles, the LUMO has substantial metal d_{z^2} character. Relativistic destabilization of the W(5d) orbitals thus explains both the higher reduction potentials and the lower energy of the near-IR transition for the Mo biscorroles.

Notes and references

[a] *Department of Chemistry and Center for Theoretical and Computational Chemistry, UiT – The Arctic University of Norway, 9037 Tromsø, Norway; E-mail: abhik.ghosh@uit.no.*

[b] *Advanced Light Source, Lawrence Berkeley National Laboratory, Berkeley, CA 94720-8229.*

† Electronic Supplementary Information (ESI) available: Crystallographic information file (cif), which has also been deposited to the Sambridge Crystallographic Data Center and assigned the deposition no. **CCDC 1534096**.

‡ *Acknowledgement.* This work was supported by the Research Council of Norway (AG) and the Advanced Light Source, Berkeley. The Advanced Light Source is supported by the Director, Office of Science, Office of Basic Energy Sciences, of the U.S. Department of Energy under Contract No. DE-AC02-05CH11231.

1. K. S. Pitzer, *Acc. Chem. Res*. **1977**, *12*, 271–276.
2. J. Autschbach, S. Siekierski, M. Seth, P. Schwerdtfeger, W. H. E. Schwarz, *J. Comput. Chem*. **2002**, *23*, 804-813.
3. (a) J. S. Thayer, in *Relativistic Methods for Chemists, Challenges and Advances in Computational Chemistry and Physics 10*, M. Barysz and Y. Ishikawa, Springer Science+Business Media B.V., 2010, pp 63-97; DOI: 10.1007/978-1-4020-9975-5_2. (b) J. S. Thayer, *J. Chem. Educ*. **2005**, *82*, 1721–1729.
4. B. A. Hess, *Relativistic Effects in Heavy-Element Chemistry and Physics*, Wiley, Chichester (UK), 2003.
5. P. Pyykkö, *Annu. Rev. Phys. Chem*. **2012**, *63*, 45-64.
6. M. Reiher, A. Wolf, *Relativistic Quantum Chemistry*, Wiley-VCH, 2015, Ch 16, pp 605-630.
7. Ilias, M.; Pershina, V. *Inorg. Chem*. **2017**, *56*, 1638−1645.
8. Relativistic effects on bond dissociation energies involving Mo and W: (a) T. Ziegler, *J. Am. Chem. Soc*. **1985**, 107, 4453-4459. (b) H. Jacobsen, G. Schreckenbach,T. Ziegler, *J. Phys. Chem.* **1994**, *98*, 11406–11410. (c) J. Li, G. Schreckenbach,T. Ziegler, *J. Am. Chem. Soc*. **1995**, *117*, 486–494. (d) Ò. González-Blanco, V. Branchadell, K. Monteyne, T. Ziegler, *Inorg. Chem*. **1998**, *37*, 1744–1748.
9. Relativistic effects on chemical and electrochemical reactivity involving Mo and W: (a) K. H. Moock, S. A. Macgregor, G. A. Heath, S. Derrick, R. T. Boeré, *J. Chem. Soc., Dalton Trans.* **1996**, 2067-2076. (b) R. Z. Liao, *J. Biol. Inorg. Chem*. **2013**, *18*, 175-181.
10. M.-S. Liao, S. Scheiner, *Chem. Phys*. **2002**, *285*, 195-206.
11. Review: A. Ghosh, *Chem. Rev.* **2017**, *117*, 3798–3881.
12. J. A. Ziegler, H. L. Buckley, J. Arnold, *Dalton Trans*. **2017**, *46*, 780-785.
13. (a) I. Nigel-Etinger, I. Goldberg, Z. Gross, *Inorg. Chem*. **2012**, *51*, 1983–1985. (b) R. Padilla, H. L. Buckley, A. L. Ward, J. Arnold, *J. Porphyrins Phthalocyanines* **2015**, *19*, 150–153.
14. R. F. Einrem, K. J. Gagnon, A. B. Alemayehu, A. Ghosh, *Chem. Eur. J.* **2016**, *22*, 517-520.
15. A. Alemayehu, K. J. Gagnon, J. Terner, A. Ghosh, *Angew. Chem. Int. Ed*. 2014, 53, 14411-14414.
16. J. H. Palmer, M. W. Day, A. D. Wilson, L. M. Henling, Z. Gross, H. B. Gray, *J. Am. Chem. Soc*. **2008**, *130*, 7786-7787.
17. A. B. Alemayehu, H. Vazquez-Lima, C. M. Beavers, K. J. Gagnon, J. Bendix and A. Ghosh, *Chem. Comm.* 2014, **50**, 11093-11096.
18. (a) A. Alemayehu, A. Ghosh, *J. Porphyrins Phthalocyanines* **2011**, *15*, 106-110. (b) Rabinovitch, E.; Goldberg, I.; Gross, Z. *Chem. Eur. J.* **2011**, *17*, 12294-12301. (c) K. E. Thomas, A. B. Alemayehu, J. Conradie, C. Beavers, A. Ghosh, *Inorg. Chem.* **2011**, *50*, 12844-12851. (d) K. E. Thomas, C. M. Beavers, A. Ghosh, *Mol. Phys.* **2012**, *110*, 2439-2444.
19. R. F. Einrem, H. Braband, T. Fox, H. Vazquez-Lima, R. Alberto, A. Ghosh, *Chem. Eur. J*. **2016**, *22*, 18747–18751.
20. A. B. Alemayehu, H. Vazquez-Lima, K. J. Gagnon, and A. Ghosh, *Chem. Eur. J*. **2016**, *22*, 6914-6920.
21. I. Johansen, H.-K. Norheim, S. Larsen, A. B. Alemayehu, J. Conradie, A. Ghosh, *J. Porphyrins Phthalocyanines* **2011**, *15*, 1335-1344.
22. A $W^{V}Cl_2$-corrole derivative, however, has been reported: R. Padilla, H. L. Buckley, A. L. Ward, J. Arnold, *J. Porphyrins Phthalocyanines* **2015**, *19*, 150–153.
23. Crystal data for Mo[T*p*CH_3PC]·CH_2Cl_2: $C_{80}H_{58}MoN_8$·CH_2Cl_2, M_r = 1312.21 g/mol, triclinic, a = 11.5246(6) Å, b = 16.3595(8) Å, c = 16.8248(9) Å, α = 78.965(3)˚, β = 86.497(3)˚, γ = 84.031(3)˚, V = 3093.8(3) $Å^3$, space group , Z = 2, θ_{max} = 35.21˚, T = 100(2) K, 858 parameters, 25 restraints, R_1 = 0.0723 (for data $I > 2\sigma(I)$), wR_2 = 0.1868 (all data).
24. All calculations were carried out with the ADF 2015 program system using fully optimized molecular geometries. Full methodological details are given in the ESI.
25. (a) G. te Velde, F. M. Bickelhaupt, E. J. Baerends, C. Fonseca Guerra, S. J. A. van Gisbergen, J. G. Snijders and T. Ziegler, *J. Comput. Chem.* **2001**, *22*, 931-967. (b) C. Fonseca Guerra, J. G. Snijders, G. te Velde and E. J. Baerends, *Theor. Chem. Acc.* **1998**, *99*, 391-403.
26. B3LYP/ZORA/STO-TZP results (gas-phase, adiabatic): IPs (eV): 5.32 ($Mo[TPC]_2$), 5.31 ($W[TPC]_2$); EAs (eV): 2.25 ($Mo[TPC]_2$), 1.96 ($W[TPC]_2$).
27. Nonrelativistic B3LYP/STO-TZP results (gas-phase, adiabatic): IPs (eV): 5.36 ($Mo[TPC]_2$), 5.31 ($W[TPC]_2$); EAs (eV): 2.28 ($Mo[TPC]_2$), 2.13 ($W[TPC]_2$).
28. M. Seth, T. Ziegler, *J. Chem. Theory Comput*. **2012**, *8*, 901-907.